Electron-Temperature Dependence of Electron-Ion Recombination in Neon*

LOTHAR FROMMHOLD,† MANFRED A. BIONDI, AND F. J. MEHR
Physics Department, University of Pittsburgh, Pittsburgh, Pennsylvania
(Received 2 August 1967)

A 3-mode microwave apparatus is used to determine electron-ion diffusion and recombination rates under conditions such that $T_+ = T_{gas} = 300°K$ and T_e is varied from 300 to 11 000°K. A high-Q cavity mode is used to ionize the gas, a second high-Q mode is used to determine the electron density during the afterglow from the change of resonant frequency of the cavity, and a nonresonant waveguide mode is used to apply a constant microwave heating field to the electrons. At $T_e = 300°K$ and $p(Ne) = 20$ Torr, a value $\alpha(Ne_2^+) = (1.7 \pm 0.1) \times 10^{-7}$ cm³/sec is obtained from analysis of the recombination-controlled electron density decays, using a computer solution of the electron continuity equation to take into account ambipolar diffusion effects. This value is in very good agreement with corrected values obtained by several other investigators. Using the same procedures, a variation of $\alpha(Ne_2^+)$ as $T_e^{-0.43}$ is found to be accurately obeyed over the range $300°K \leqslant T_e \leqslant 11\,000°K$, suggesting that the initial capture step is rate-limiting in the dissociative recombination process.

I. INTRODUCTION

THERE is a considerable body of experimental information[1–4] demonstrating that the capture of thermal (~300°K) electrons by molecular ions such as Ne_2^+, N_2^+, O_2^+, and NO^+ is characterized by very large capture cross sections, $Q_{rec} > 10^{-14}$ cm². There is an even larger body of measurements[5–10] yielding large recombination rates in gases in which the ions have not been mass-identified but are expected to be molecular in character. In the cases of neon and argon, the capture process has been shown to be dissociative recombination,[11,12] i.e.,

$$XY^+ + e \rightarrow (XY)_{\text{unstable}}^* \rightarrow X^* + Y, \qquad (1)$$

where the superscripts + and * indicate ionized and electronically excited states, respectively. It is, therefore, reasonable to suppose that the dissociative process is responsible for the large two-body recombination coefficients observed in the other cases, inasmuch as no other two-body process has been suggested which provides a sufficiently large capture cross section.

Theoretical calculations[13–16] have, until recently, been at best qualitative in estimating the dissociative capture cross section and its dependence on the incident electron energy; inasmuch as an *ab initio* calculation requires detailed knowledge of the wave functions of the molecular and atomic states indicated in reaction (1), from which must be calculated the potential-energy curves and autoionization probabilities as a function of the internuclear separation of the atoms. Recently, calculations of the rate of recombination of electrons and H_2^+, He_2^+, N_2^+, and O_2^+ have appeared,[15,16] leading to values in reasonable agreement with the experimental results for N_2^+ and O_2^+.

We have undertaken measurements of the dependence of the recombination coefficients on electron temperature in order to provide information which may be compared with theory as results of calculations become available. In addition, in the ionosphere, where dissociative recombination is believed to be one of the important electron removal processes, the electrons often have temperatures elevated with respect to the ions and neutral molecules; therefore, our experiment provides a means of more closely duplicating upper atmosphere conditions in our laboratory studies of recombination involving ionospheric ions.

In the following sections we discuss the microwave-heating technique as applied to afterglow studies, describe the three-mode microwave apparatus used for the measurements, and present the results of the studies of electron density decay in Ne afterglows. The results are analyzed in terms of recombination and ambipolar diffusion rates as a function of electron temperature and finally are compared with results of other investigators.

* This research was supported, in part, by the Defense Atomic Support Agency and the U. S. Army Research Office (Durham), under contract Nos. DA-31-124-ARO-D-G-518.

† Present address: Physics Department, University of Texas, Austin, Tex.

[1] W. H. Kasner and M. A. Biondi, Phys. Rev. **137**, A317 (1965).
[2] R. C. Gunton and T. M. Shaw, Phys. Rev. **140**, A748 (1965); **140**, 756 (1965).
[3] W. H. Kasner, Phys. Rev. (to be published).
[4] C. S. Weller and M. A. Biondi, Phys. Rev. Letters **19**, 59 (1967).
[5] M. A. Biondi and S. C. Brown, Phys. Rev. **76**, 1697 (1949).
[6] H. Oskam, Philips Res. Rept. **13**, 401 (1958).
[7] M. A. Biondi, Phys. Rev. **129**, 1181 (1963).
[8] R. D. Thomas, R. Hackam, and J. J. Lennon, in *Proceedings of the Seventh International Conference on Ionization Phenomena in Gases, Belgrade, 1965*, edited by B. Perovic and D. Tosic (Belgrade, 1966), Vol. I, p. 27 ff.
[9] H. Oskam and V. R. Mittelstadt, Phys. Rev. **132**, 1435 (1963); **132**, 1445 (1963).
[10] W. Hess, Z. Naturforsch. **20a**, 451 (1965).
[11] T. R. Connor and M. A. Biondi, Phys. Rev. **A140**, 778 (1965).
[12] L. Frommhold and M. A. Biondi, Bull. Am. Phys. Soc. **11**, 493 (1966).
[13] D. R. Bates, Phys. Rev. **77**, 718 (1950); **78**, 492 (1950); **82**, 103 (1951).
[14] E. Bauer and T. Y. Wu, Can. J. Phys. **34**, 1436 (1956).
[15] R. L. Wilkins, J. Chem. Phys. **44**, 1884 (1966).
[16] C. S. Warke, Phys. Rev. **144**, 120 (1966).

II. PRINCIPLE OF THE EXPERIMENT

A. Afterglow Decay Analysis

The recombination coefficients are determined from measurements of the decay of electron density with time following removal of external ionizing sources (afterglow period). On the assumption that the electrons quickly achieve a stationary energy distribution in the afterglow, their density variation may be described by the continuity equation

$$\partial n_e/\partial t=\sum_i P_i-\sum_j L_j-\nabla\cdot\mathbf{\Gamma}_e, \tag{2}$$

where n_e is the electron density and P_i and L_j are the various rates of volume ionization and electron removal, respectively; for example, metastable-metastable ionization and electron-ion recombination. The electron-particle current density $\mathbf{\Gamma}_e$ describes such processes as ambipolar diffusion to the boundaries of the ionized-gas container.

In the present Ne studies care is taken to achieve conditions in the afterglow where all volume production terms are negligible ($\sum P_i\approx 0$), the only important volume-loss term is two-body electron-ion recombination, and there is only one positive-ion species present and no negative ions. In this case we may write

$$L_{\text{rec}}=\alpha n_e n_+\simeq\alpha n_e^2, \tag{3}$$

where α is the two-body recombination coefficient and we have used the requirement of space charge neutrality to set $n_+\simeq n_e$. If ambipolar diffusion is the only important electron-flow term, we have $\mathbf{\Gamma}_e=-D_a\nabla n_e$, where D_a is the ambipolar diffusion coefficient, given by[17]

$$D_a=D_+(1+T_e/T_+), \tag{4}$$

D_+ being the positive-ion diffusion coefficient, T_e and T_+ the electron and ion "temperatures," respectively. Equation (2) then becomes

$$\partial n_e/\partial t\simeq-\alpha n_e^2+D_a\nabla^2 n_e. \tag{5}$$

In some cases it is possible to achieve conditions where the diffusion term is very small compared to the recombination-loss term, leading to the well-known "recombination" solution of Eq. (5)

$$1/n_e=1/n_{e0}+\alpha t. \tag{6}$$

In the present studies, although diffusion loss is very small when $T_e\simeq 300°\text{K}$, as the electron temperature is raised by microwave heating, the ambipolar diffusion increases in accordance with Eq. (4) and the full Eq. (5) is required to describe the electron decay.

[17] See, for example, M. Schottky, Physik Z. **25**, 635 (1924); M. A. Biondi, Phys. Rev. **93**, 1136 (1954). In cases where the electron energy distribution is not Maxwellian, Eq. (4) may be rewritten as $D_a=D_+(1+k\bar{u}_e/\bar{u}_+)$, where $\bar{u}_e$ and $\bar{u}_i$ are the average electron and ion energies, respectively, and k is a coefficient (of the order of unity) which depends on the forms of the energy distributions.

This nonlinear differential equation has been solved numerically by Oskam[6] for infinite plane parallel geometry and by Gray and Kerr[18] for the infinite cylinder and the sphere. We have developed a computer program applicable to solution of Eq. (5) for geometries having cylindrical symmetry.[19] We use the program to calculate the reciprocal of a special average of the electron density (see Sec. II B) as a function of time in the afterglow, inserting in the computations several possible initial spatial distributions for the electrons (see Sec. IV B) and known values of D_+, T_e, and T_+. We then treat α, the desired recombination coefficient, as a parameter to obtain the best fit to the experimental data.

B. Electron-Density Determinations

The method of determining average electron densities from measurements of the change of resonant frequency of a microwave cavity enclosing the ionized gas has been described in detail elsewhere[20]; therefore, we discuss only the particular features relevant to the present work. At low electron densities the imaginary part of the conductivity at a point in an ionized gas is linearly proportional to the electron concentration. Thus, the perturbation-theory result for the change of resonant frequency Δf_0 of a microwave cavity surrounding the ionized gas may be written[20] as

$$\Delta f_0=C\int_{\text{vol}} n_e(\mathbf{r},t)E^2(\mathbf{r})dV\Big/\int_{\text{vol}} E^2(\mathbf{r})dV, \tag{7}$$

where C represents a group of known physical constants and $\mathbf{E}(\mathbf{r})$ is the probing microwave electric field in the cavity, and the integrations are carried over the cavity volume.

In the present work we display the decay of electron density in terms of a "microwave averaged" density $\bar{n}_{\mu w}(t)$, namely,

$$\bar{n}_{\mu w}(t)\equiv\int_{\text{vol}} n_e(\mathbf{r},t)E^2(\mathbf{r})dV\Big/\int_{\text{vol}} E^2(\mathbf{r})dV=\Delta f_0/C. \tag{8}$$

The use of the microwave averaged density permits us to plot, in effect, a directly measured quantity without making assumptions concerning the spatial distribution of the electrons in the cavity. The computer solution of Eq. (5) for $n_e(\mathbf{r},t)$ is then averaged over the cavity according to Eq. (8) to yield values of $\bar{n}_{\mu w}(t)$ for comparison with our measurements.

C. Electron Heating by Microwaves

In order to maintain as simple an analysis of the afterglow as possible, it is necessary that the electron energy distribution maintain a stationary value through-

[18] E. P. Gray and D. E. Kerr, Ann. Phys. (N. Y.) **17**, 276 (1959).
[19] L. Frommhold and M. A. Biondi (to be published).
[20] M. A. Biondi, Rev. Sci. Instr. **22**, 500 (1951).

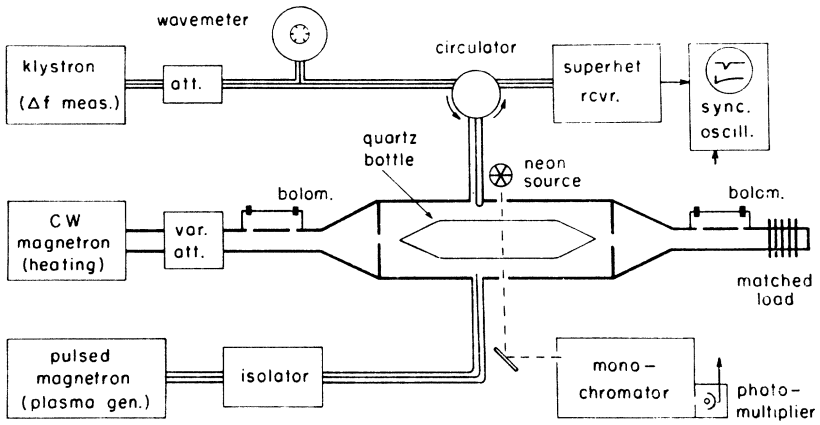

FIG. 1. Simplified block diagram of three-mode microwave afterglow apparatus employing microwave heating of the electrons in the ionized gas.

out the afterglow; otherwise, the simple coordinate space continuity equation, Eq. (2), will involve time-varying recombination and diffusion coefficients, α and D_a. To this end, steps have been taken to assure that a constant microwave heating field is applied to the electrons, with the result that a stationary energy distribution at some electron "temperature" T_e is expected.

Margenau[21] has shown that the velocity distribution function f_0 of electrons in a gas in the presence of an applied microwave heating field is given by

$$f_0=\exp\left\{-\int_0^{v^2}\frac{(m/2)d(v^2)}{kT+[\frac{1}{6}M\gamma^2l^2/(v^2+\omega^2l^2)]}\right\}, \quad (9)$$

provided that the collisions are predominantly elastic. Here, m and M are the masses of electrons and neutrals, respectively, T is the ambient temperature, $\gamma=eE_m/m$ is the acceleration of the electrons due to the amplitude of the electric field E_m, l denotes the electron mean free path, and ω is the microwave radian frequency. From this distribution function, a mean energy $\bar{\epsilon}$ has been derived for the case of weak fields and constant mean free path (approximately obeyed over this energy range in Ne),

$$\bar{\epsilon}=\tfrac{3}{2}kT+(M/4\omega^2)\gamma^2. \quad (10)$$

Margenau points out that this formula may be applied from zero fields up to a field strength for which the second term in the equation for $\bar{\epsilon}$ is equal to $\frac{3}{2}kT$, i.e.,

$$E_0\leqslant(m/e)\omega(6kT/M)^{1/2}. \quad (11)$$

Thus, electron "temperatures" may be evaluated for mean energies between $\frac{3}{2}kT$ and $3kT$ by using Eq. (10).

For high fields (but still predominantly elastic collisions) kT may be ignored in the denominator of Eq. (9). Provided the mean free path l is not strongly dependent upon the electron velocity, as is the case for electrons in neon, Eq. (9) may be rewritten in an integrated form. The expression for the mean energy $\bar{\epsilon}$ thus found is used to evaluate the mean energy for this case, leading to the result

$$\bar{\epsilon}=(M/4\omega^2)\gamma^2F(z), \quad (12)$$

where $z=(3m/M)^{1/2}(k\omega^2/\gamma)$ and $F(z)=zU(2,z)/U(1,z)$. Here, the $U(n,z)$ are Weber parabolic cylinder functions.[22] A graph of the function $F(z)$ is given in Fig. 6 of Appendix A. For very low values of z, i.e., where $F(z)$ increases linearly with z, the resulting distribution function is essentially Druyvesteynian, E/p is the controlling parameter and the mean electron energy becomes pressure-dependent. For values of z above 1 [$F(z)$ nearly constant], the resulting distribution function is nearly Maxwellian, the neutral pressure is unimportant and the determining quantity for the electron energy is E/ω rather than E/p. This "low-pressure case" is the only one of importance in our experiments, inasmuch as our z values are mostly well above 1.

It is of interest to note that, for such large z values, Eq. (12) agrees with Eq. (10) after the $\frac{3}{2}kT$ term (which is a small quantity according to our assumptions) has been added, because $F(z)$ assumes the value 1 in this case. Accordingly, we have used Eq. (10) over the whole range of heating fields whenever the function $F(z)$ is sufficiently close to unity. When $F(z)$ begins to deviate from unity by more than 5%, an approximate expression,

$$\bar{\epsilon}\simeq\tfrac{3}{2}kT+(M/4\omega^2)\gamma^2F(z), \quad (13)$$

is used. Whenever Eq. (13), which is merely a reasonable interpolation formula, has been employed, the quantity $\frac{3}{2}kT$ is indeed small enough so that the result of Eq. (12) does not differ by more than 10% from the results of Eq. (13).

Summarizing, the temperature measurements can be made with a theoretically estimated accuracy of some few percent by measuring the continuous-wave heating power by means of the directional couplers and bolometers (see Fig. 1). For the TE_{11} mode employed, an

[21] H. Margenau, Phys. Rev. **69**, 508 (1946).

[22] M. Abramowitz and I. A. Stegun, *Handbook of Mathematical Functions*, edited by M. Abramowitz and I. A. Stegun (Dover Publications, Inc., New York, 1964).

electrical field amplitude is derived from the power measurement by well-known relationships.[23]

In the circular-waveguide mode, the microwave heating-field strength depends on position; therefore, the energy input to the electron gas varies over the plasma volume. However, within the ambipolar space-charge potential well, the electron gas displays a very-high heat conductivity as a result of the large electron free diffusion rate. We therefore expect that the electrons are nearly isothermal within the plasma container, the electron "temperature" being determined by a balance between the average rate of energy input to the electron gas from the microwaves and the rate of energy loss by the electrons to the neutral gas as a result of collisions. Since the input at each point in space is proportional to $\sigma_r E_m^2$ (where σ_r, the real part of the electrons' conductivity, is proportional to n_e), the appropriate microwave field to use in Eqs. (10), (12), or (13) is

$$\langle E_m^2\rangle_{\rm av}=\int_{\rm vol} n_e(\mathbf{r})E_m^2(\mathbf{r})dV \Big/ \int_{\rm vol} n_e(\mathbf{r})dV, \quad (14)$$

where $E_m(\mathbf{r})$ represents the microwave heating-field strength and the integral is carried over the volume of the plasma container. In the present case, in which the plasma-container diameter is 41% of the circular-waveguide diameter, we find that $\langle E_m^2\rangle_{\rm av}$ lies between $0.87E_m^2(0)$ and $0.91E_m^2(0)$, where $E_m(0)$ is the microwave field intensity at the center of the waveguide, depending on the precise form of the electron density distribution in the plasma container. (The above values correspond to a uniform and a fundamental diffusion mode distribution of electrons, respectively.) During most of the afterglow the spatial distribution of the electrons is such that the latter value, $0.91E_m^2(0)$, is nearly correct; therefore, we have used it to evaluate the electron temperature.

III. EXPERIMENTAL APPARATUS

The over-all apparatus is shown in a simplified block diagram in Fig. 1, while the dual-mode cavity/circular waveguide structure is shown in more detail in Fig. 2. The gas sample under study is introduced from an ultrahigh-vacuum gas handling system[24] into a thin-walled cylindrical quartz bottle with conical tapers at each end to minimize microwave field distortion. The microwave structure enclosing the quartz bottle operates in three modes: a high-Q TE_{111} or TM_{010} cavity mode used to ionize the gas, a high-Q TM_{010} cavity mode used to measure the detuning of the cavity by the electrons and so determine the electron density, and a nonresonant TE_{11} circular-waveguide mode for application of the microwave heating field.

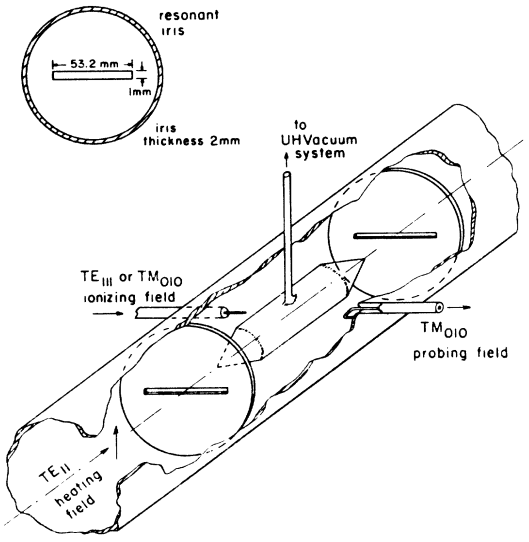

FIG. 2. Cutaway view drawing of cylindrical cavity-waveguide section bounded by resonant irises.

The waveguide/cavity cylinder is 3.65 cm in radius and the resonant cavity is formed by closing off the ends with flat disks spaced 29.2-cm apart, giving resonant frequencies in the 3-Gc/sec range. Resonant coupling irises,[25] as shown in the upper left of Fig. 2, are cut in these disks to permit propagation of the travelling-wave heating field along the waveguide. At the resonant frequency, 2.68 Gc/sec, of the irises the heating wave is transmitted without detectable reflection by the irises or by the quartz bottle.

The irises do not affect the Q's of the cavity modes, since the slots are parallel to the wall current flows for the modes employed. In this manner a high unloaded Q (measured value ~20 000) is obtained in the TM_{010} mode, permitting accurate electron detuning measurements to be made, while the presence of the electrons in the ionized gas does not appreciably modify the travelling wave heating field at 2.68 Gc/sec. Inasmuch as the resonant irises distort the field in their vicinity, sufficient space is allowed between irises and quartz bottle to yield essentially the waveguide's fundamental mode field over the region of the bottle. (The next higher mode is "damped" 6 dB/cm as one moves away from the iris, with higher modes falling off even more rapidly.)

The gas is ionized by a pulse of power (pulse length adjustable from ~10 μsec to ~5 msec) from a 4J62 magnetron buffered from the cavity by a ferrite isolator. The pulses are repeated between 10 and 100 times per second. The resonant frequency shift of the cavity during the afterglow is determined in the conventional way,[20] using a very low-energy (<2 μW) probing signal

[23] N. Marcuvitz, *Waveguide Handbook*, edited by N. Marcuvitz (McGraw-Hill Book Co., Inc., New York, 1947), Vol. 10, pp. 66 ff.
[24] See, for example, D. Alpert, in *Handbuch der Physik*, edited by S. Flugge (Springer-Verlag, Berlin, 1957), Vol. 12.
[25] C. G. Montgomery, R. H. Dieke, and E. M. Purcell, *Principles of Microwave Circuits* (McGraw-Hill Book Co., New York, 1947), Vol. 8, p. 171; T. Moreno, *Microwave Transmission Design Data* (Dover Publications, Inc., New York, 1948), p. 157.

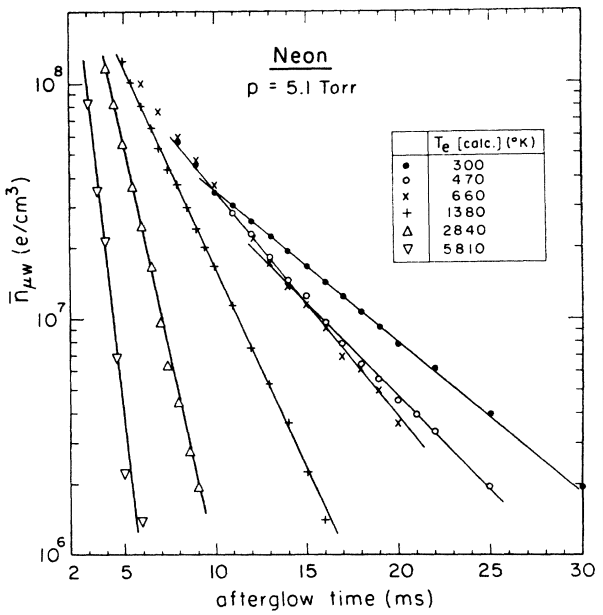

FIG. 3. Measured electron density decays during the afterglow at $T_+=T_{gas}=300°K$ for various electron temperatures. The indicated values of T_e are calculated from the measured microwave heating field strengths as described in Sec. II C.

from a 726B klystron, measuring its frequency with a high-Q cavity wavemeter and observing its reflection from the cavity with a sensitive superheterodyne receiver and oscilloscope whose sweep is synchronized with the magnetron pulse. By noting the time of minimum power reflection for a given incident probing frequency, one determines the cavity's resonant frequency at that instant. By successively using different frequencies and noting the corresponding times of minimum reflection, one obtains the curve of resonant frequency shift Δf_0 versus time and hence can compute $\bar{n}_{\mu w}(t)$ according to Eq. (8).

The microwave heating field is supplied by a 4J62 magnetron-operated cw and tuned to the frequency 2.68 Gc/sec, at which the resonant irises are nonreflecting. The field strength in the guide is adjusted by a variable attenuator and monitored by precisely calibrated directional couplers and bolometers in the rectangular-waveguide sections. Transformation from the rectangular to the circular waveguide is accomplished by exponentially tapered sections, which introduce negligible reflection. The travelling-wave heating field is absorbed in a matched load at the end of the waveguide line. From the known insertion losses of the directional couplers and the bolometer power readings, one calculates the energy density in the waveguide and hence the heating-field strength.

TABLE I. Comparison of electron temperatures calculated from the microwave heating-field strength and inferred from the effect on the ambipolar diffusion rate, as measured in Fig. 3.

T_e (calc) (°K)	τ_f (calc) (msec)	τ_f (meas) (msec)	T_e (inferred) (°K)
300	6.7	6.7±0.1	300±10
470	5.2	5.4±0.1	445±15
660	4.2	4.5±0.2	597±40
1380	2.4	2.6±0.1	1250±50
2840	1.3	1.3±0.1	2800±250
5810	0.66	0.6–0.7	5470–6420

In addition to the microwave measurements of the electron behavior we wish to observe the Ne metastable atoms, which can contribute significant ionization as a result of metastable-metastable collisions. In order to monitor the Ne metastable atom concentrations during the afterglow, radiation from a capillary or a glow discharge Ne source is transmitted through the center of the quartz bottle, dispersed by a monochromator, and a particular transmitted line's intensity (e.g., λ6402, which terminates on the lower Ne metastable level) detected by a photomultiplier, whose output is applied to the synchronized oscilloscope (see Fig. 1). In this manner the time-varying optical absorption by metastable atoms in the ionized gas is observed during the afterglow.

Finally, several small ports are drilled along a line parallel to the axis of the cylinder to permit observation, via a light pipe and monochromator, of the axial distribution of the radiation *emitted* from the discharge and the afterglow.

IV. MEASUREMENTS

A. Ambipolar Diffusion

In order to test the apparatus for proper operation and to check the values of the electron temperatures calculated from the microwave heating fields, we have carried out afterglow studies of ambipolar diffusion in Ne. Here we have used electron densities and neutral gas pressures sufficiently low that ambipolar diffusion is the principal electron-loss process, yet the gas pressure (~5 Torr) is sufficiently high that the predominant afterglow ion is expected to be Ne_2^+. Under these conditions the first term on the right of Eq. (5) may be neglected and one obtains a solution in terms of a sum of exponentially decaying diffusion modes, the longest lived of which is the fundamental mode, whose decay time constant is given by $\tau_f=\Lambda_f^2/D_a$. (Λ_f is the fundamental diffusion length of the tapered cylinder and has the value 0.61 cm; see Appendix B.) Thus, at late times in the afterglow we expect a simple exponential decay of electron density with time constant τ_f. That such is the case is indicated by the data of Fig. 3, taken at a Ne pressure of 5.1 Torr and a gas temperature of 300°K.

According to Eq. (4), D_a increases with increasing T_e (we expect that D_+ and T_+ remain fixed under microwave heating, inasmuch as neither the neutral gas density nor the neutral or ion temperature is altered), leading to a corresponding decrease in τ_f. Using the value $D_+p=140$ cm^2/sec Torr for Ne_2^+ ions in Ne ob-

tained from ion mobility[26] and from afterglow[9] measurements at 300°K, and the values of T_e calculated from the microwave heating field strength, we obtain the comparison between theoretical and measured decay rates and between calculated and inferred electron temperatures given in Table I. The rather good agreement between calculated and experimental values suggests that our electron temperature scale, derived from the microwave heating field, is accurate to within ~10% over the range 300–6000°K.

B. Electron-Ion Recombination

By increasing the neutral-gas density and the initial electron density in the afterglow, the recombination term in Eq. (5) becomes predominant, especially at low values of T_e, so that initially the reciprocal of the electron density should increase approximately linearly with time, as predicted by Eq. (6). At the higher plasma densities, however, one must be certain that the heating wave is not appreciably absorbed or reflected in order that our calculations of T_e be accurate. It is found that ~200 μsec after the end of the ionizing pulse only a few percent of the heating power is reflected from and absorbed by the plasma, and that the reflection and absorption decrease to unmeasurably small levels at 400 μsec in the afterglow, so that T_e should be constant and equal to the calculated value throughout the afterglow.

In order that our observed electron-density decays may be compared with the computer solution of Eq. (5) we have adjusted the discharge conditions (pulse length and repetition rate) to minimize the metastable atom concentration, as observed by the optical-absorption apparatus, at the start of the afterglow. In this way metastable-metastable ionization is made negligibly small during the whole afterglow. The observed electron density decays at $p=20$ Torr of Ne are shown in Fig. 4, which presents measured values of $1/\bar{n}_{\mu w}$ versus t for $T_+=T_{gas}=300$°K and different values of T_e. The time zero point (start of afterglow) has been displaced for the various curves for clarity.

As noted earlier, to obtain the computer solutions for comparison with the data, the known values of T_{gas}, T_+, T_e, and D_+ are inserted into Eqs. (4) and (5) and various values of α are tried in obtaining the best fit of the solutions to the data. The first trial values of α are determined from the initial slopes of the $1/\bar{n}_{\mu w}$-versus-t curves.

An added parameter in the computer solutions is the initial form of the electrons' spatial distribution. We have found that, for the three initial distributions which almost certainly include our experimental conditions, the computed $1/\bar{n}_{\mu w}$-versus-t curves follow rather closely the same form after a few hundred μsec. The three initial spatial distributions tried are the fundamental diffusion mode distribution raised to the zeroth, first, and second powers. [The fundamental mode distribution is obtained by computer solution of Eq. (5) with α set equal to zero, and n_e taken as zero on the boundaries of the tapered cylinder.] These distributions may be approximately represented by

$$n_e(r,z,0)=n_0[J_0(2.4r/R)\cos(2\pi z/L_{eff})]^k, \quad (15)$$

where L_{eff} is the effective length of the tapered cylinder (see Appendix B), R its radius, and where $k=0$, 1, 2. For $k=0$, we have the uniform spatial distribution often assumed in recombination analyses; $k=1$ represents a "fundamental diffusion mode" distribution for the starting density; and $k=2$ represents an initial plasma distribution somewhat constricted toward the center of the cylinder both radially and axially. The observed recombination radiation emitted from the early afterglow suggests that the actual initial electron distribution is approximated by a value of k between 1 and 2.

The computer solutions shown in Fig. 4 are obtained with an initial electron spatial distribution of the "fundamental diffusion mode" ($k=1$) type. Rather good agreement between observed and predicted behavior is obtained, even when the electron decay departs from the linear $1/n_e$ recombination controlled region

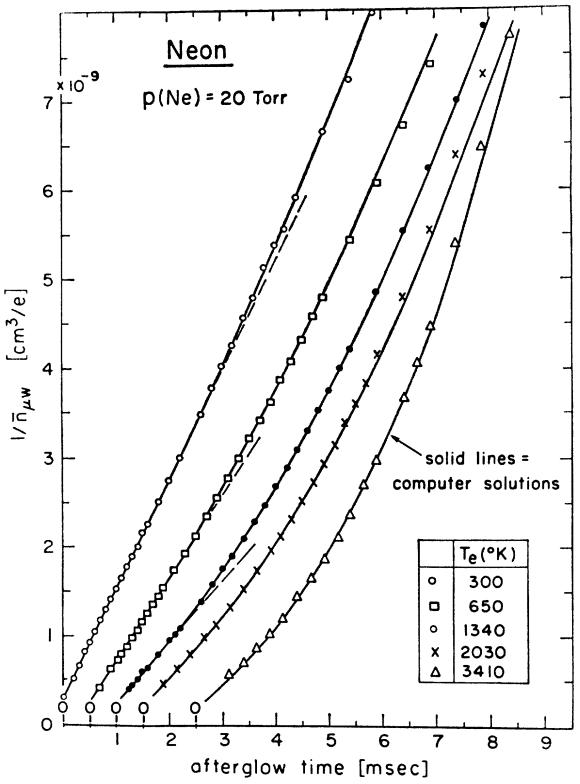

FIG. 4. Recombination and diffusion loss of electrons during the afterglow displayed by plotting $1/\bar{n}_{\mu w}$ versus t. The electron temperature is varied while $T_+=T_{gas}=300$°K. (The time zero point has been displaced for the various curves for clarity.) The solid lines represent computer solutions of Eq. (5) using α as a parameter to obtain best fits to the data (see text for details).

[26] L. M. Chanin and M. A. Biondi, Phys. Rev. **106**, 473 (1957).

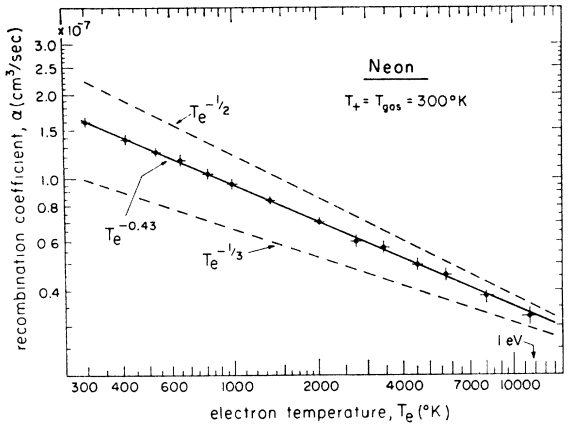

FIG. 5. Measured variation of the recombination coefficient, $\alpha(Ne_2^+)$, as a function of electron temperature. The solid line through the points represents a $T_e^{-0.43}$ variation, while the dashed lines indicate the slopes of $T_e^{-1/3}$ and $T_e^{-1/2}$ dependences.

(dashed lines) as a result of the increasing importance of ambipolar diffusion loss.

The values of α inferred from the computer solution fits to the observed decay curves are shown as a function of T_e in Fig. 5, which presents the data on a log-log plot. The error bars are intended to indicate the extreme values of α which provide a possible fit to the decay curves of Fig. 4 and thus do not include such systematic errors in α as may arise from calibration errors in determining the absolute values of n_e. The dashed lines show variations of α as $T_e^{-1/2}$ and $T_e^{-1/3}$, while the solid line through the points represents a variation of α as $T_e^{-0.43}$. At $T_e=T_+=T_{gas}=300°K$ a value $\alpha(Ne_2^+)=(1.7\pm0.1)\times10^{-7}$ cm³/sec is obtained, as the average of several runs, in satisfactory agreement with the results of other investigations (see Sec. V).

V. DISCUSSION AND CONCLUSIONS

The present results may be compared with the results of other investigations in two principal respects: (a) the absolute value of $\alpha(Ne_2^+)$ at $T=300°K$, and (b) the dependence of α on T_e. In the former case, there are a number of results, extending back to 1949, which are sufficiently accurate to warrant comparison, while in the latter case, there are only two rather recent results which can be considered to give reliable temperature dependences of the recombination coefficient.

Biondi and Brown[5] obtained the value $\alpha(Ne_2^+)=2.1\times10^{-7}$ cm³/sec at 300°K and $p=29.3$ Torr in the original investigation of Ne afterglows using microwave techniques; however, they assumed a uniform spatial distribution of the electrons in the ionized gas throughout the afterglow, and therefore their results require correction for the actual spatial distribution resulting from diffusion. Applying our computer solution to their cylindrical plasma container ($R=1.9$ cm, $L=2.5$ cm) in a TM_{010} cavity ($R_c=3.5$ cm, $L_c=3.8$ cm), we obtain a corrected value from their data, $\alpha_{corr}=1.7\times10^{-7}$ cm³/sec, in very good agreement with our results at $T_e=T_+=T_{gas}=300°K$.

Oskam[6] obtained an uncorrected value $\alpha=2.3\times10^{-7}$ cm³/sec at 20 Torr in a cylinder ($R=1.15$ cm, $L=3.9$ cm), leading to a value $\alpha_{corr}=1.8\times10^{-7}$ cm³/sec when our computer solution is applied to correct for the actual spatial distribution of the electrons. Recently, Oskam and Mittelstadt[9] obtained an uncorrected value $\alpha=2.2\times10^{-7}$ cm³/sec at 35 Torr; we obtain a value $\alpha_{corr}=1.8\times10^{-7}$ cm³/sec using our computer solution adapted to their TE mode microwave field distribution.

Biondi[7] obtained an uncorrected value $\alpha=3.4\times10^{-7}$ cm³/sec at 23 Torr in a cylinder ($R=2.22$ cm, $L=3.82$ cm). Gray and Kerr's corrections for a spherical container were applied to the cylindrical case by taking a sphere of equal Λ_f(0.735 cm). For an initial fundamental mode diffusion distribution one obtains a corrected value $\alpha_{corr}=1.9\times10^{-7}$ cm³/sec, which is, however, somewhat uncertain in view of the large correction factor.

Recently, Connor and Biondi[11] carried out afterglow measurements in a smaller plasma container (a sphere with $\Lambda_f=0.19$ cm) at an order-of-magnitude higher electron density than in these other studies. They obtained an uncorrected value $\alpha=2.8\times10^{-7}$ cm³/sec at $p=68$ Torr, which yielded a corrected value $\alpha=2.0\times10^{-7}$ cm³/sec, in satisfactory agreement with the present results and indicates the predominance of two-body dissociative recombination even at the higher plasma densities ($n_e\sim10^{10}$–10^{11} cm^{-3}).

The measurements of Hess,[10] to be discussed in more detail later, yield an uncorrected value of $\alpha=2.0\times10^{-7}$ cm³/sec at $p=20$ Torr in a long cylinder with $\Lambda_f=0.62$ cm. When our computer corrections are applied, one obtains a value $\alpha_{corr}\simeq1.7\times10^{-7}$ cm³/sec at $T_e=T_+=T_{gas}=300°K$, in good agreement with the present results.

Very recently, Kasner[3] has demonstrated that the two-body recombination observed in Ne afterglows at $p\sim20$ Torr involves Ne_2^+ ions by use of a microwave/mass spectrometer apparatus. His studies, carried out in a rectangular parallelepiped cavity which the ionized gas can fully occupy, lead to an uncorrected value $\alpha=2.3\times10^{-7}$ cm³/sec at 300°K. Using our computer solution adapted to rectangular parallelepiped geometry, we find that Kasner's corrected value is $\alpha_{corr}=1.8\times10^{-7}$ cm³/sec, in good agreement with our results.

As noted earlier, our results are fully corrected for the effects of diffusion by use of our computer solutions. Any error in the value of α must come from an error in the determinations of the absolute electron-density values or of afterglow time intervals. (Metastable ionizing effects on the decay curves are minimized by working at minimum afterglow metastable concentrations, as monitored by the optical-absorption apparatus.) It is interesting that the presence of the quartz bottle within the cavity disturbs the microwave field in such a way that we overestimate n_e values slightly and therefore

TABLE II. Comparison of various experimental values of $\alpha(Ne_2^+)$ at $T_e=T_+=T_{gas}=300°K$.

Investigators	Container	Dim. (cm)	Typical p(Ne) (Torr)	Uncorrected "α" (cm³/sec)	Corrected α_{cor} (cm³/sec)	Correction method
Biondi and Brown[a]	Cylinder	$R=1.9$ $L=2.5$	29	2.1×10^{-7}	1.7×10^{-7}	Present computer solution
Oskam[b]	Cylinder	$R=1.15$ $L=3.9$	20	2.3×10^{-7}	1.8×10^{-7}	Present computer solution
Biondi[c]	Cylinder	$R=2.22$ $L=3.82$	24	3.4×10^{-7}	1.9×10^{-7}	Gray and Kerr,[h] adapted for finite cylinder
Oskam and Mittelstadt[d]	Cylinder	$\Lambda_f=0.63$	35	2.2×10^{-7}	1.8×10^{-7}	Present computer solution for TE mode
Connor and Biondi[e]	Sphere	$R=0.60$ $\Lambda_f=0.19$	68	2.8×10^{-7}	2.0×10^{-7}	Gray and Kerr[h] correction for sphere
Hess[f]	Long cylinder	$\Lambda_f=0.62$	20	2.0×10^{-7}	1.7×10^{-7}	Present computer solution
Kasner[g]	Rectangular parallelepiped	$L_x=5.00$ $L_y=8.00$ $L_z=6.41$	20	2.3×10^{-7}	1.8×10^{-7}	Modification of present computer solution for rectangular geometry
Present work	Tapered cylinder	$R=1.5$ $L_{eff}=9.1$	20	...	$(1.7\pm0.1)\times10^{-7}$	Present computer solution

[a] See Ref. 5. [b] See Ref. 6. [c] See Ref. 7. [d] See Ref. 9. [e] See Ref. 11. [f] See Ref. 10. [g] See Ref. 3. [h] See Ref. 18.

underestimate α. We have minimized this error by using the thinnest quartz walls practicable. Those other experiments with quartz bottles suffer from the same criticism, while studies such as Kasner's are free of this defect. Thus, it appears from a study of Table II that the recombination coefficient for Ne almost certainly has the value $\alpha(Ne_2^+)=(1.7\pm0.2)\times10^{-7}$ cm³/sec at $T_e=T_+=T_{gas}=300°K$.

There have been few determinations of the temperature dependence of $\alpha(Ne_2^+)$ which are sufficiently reliable to warrant comparison with the present results. The principal methods employed have made use of cooling and heating of the whole cavity to vary T_{gas} and, therefore, T_e and T_+ as well, of "afterglow quenching" in which the effect of a microwave electron heating pulse is noted on the afterglow recombination radiation intensity, and of the effect of microwave electron heating on the rate of loss of electrons during the afterglow.

We do not consider the "afterglow quenching" method to give a reliable estimate of the variation of $\alpha(Ne_2^+)$, inasmuch as dissociative recombination into a given radiating atomic state depends critically on the nature of the curve crossing between the molecular ion potential curve and that of the unstable molecule which, on dissociation, gives rise to the given atomic state. Thus, the intensity I_{ij} of a particular afterglow line representing a transition between states i and j of Ne depends on α_i, the partial recombination coefficient for production of the ith atomic state. Since the α_i's for different upper states should be widely different in their magnitudes and their dependences on T_e as a result of the curve crossing problem, no observation of total (undispersed) afterglow recombination intensity or of a given afterglow line intensity can be regarded as giving the dependence of the total coefficient $\alpha(Ne_2^+)$ on T_e, especially if some of the states produced are nonradiating metastable states.

Thus, the T_e dependences of $\alpha(Ne_2^+)$ reported by Farhat[27] ($\alpha\sim T_e^{-0.9}$) and by Nygaard[28] ($\sim T_e^{-1.4\pm0.2}$) on the basis of analyses of afterglow quenching measurements can not be considered as reliable. It is interesting to note, however, that Taylor and Herskovitz,[29] whose data Farhat analyzed, dispute Farhat's conclusions and obtain a variation as $T_e^{-0.5}$ to $T_e^{-0.66}$, in fair agreement with the present results.

The study by Hess[10] of the effect on the electron loss rate of application of a time-varying microwave heating field during the afterglow provides a more direct measurement of the variation of $\alpha(Ne_2^+)$ with T_e. Unfortunately, the analysis of the afterglow is complicated by the fact that one has time varying coefficients D_a and α to contend with in the solution of Eq. (5). As a result, Hess was led to several approximations in his analysis: that (a) the increase of T_e above T_{gas} is linearly proportional to the microwave power absorbed, (b) the actual microwave absorption as the cavity resonance passes through the heating frequency is reasonably approximated by a linearly increasing function of time, and (c) the variation of $\alpha(Ne_2^+)$ follows a simple power-law dependence on T_e. Although the errors in the first two assumptions do not seem negligible, we are unable to assess quantitatively their effect on Hess's analysis. He obtains a variation as $T_e^{-0.25}$ for $300°K<T_e<600°K$ and as $T_e^{-0.4}$ for $900°K<T_e<2400°K$, although the large scatter in the data appears to admit variations between powers of -0.35 and -0.45 in the 900–2400°K range. In view of the approximations in Hess's analysis, the agreement with the present results is satisfactory over the 900–2400°K range.

Finally, studies have been carried out in which the gas temperature (and hence T_e and T_+) has been varied. Biondi and Brown[5] carried out such studies over the range 77–420°K and found essentially no variation of

[27] N. H. Farhat, Proc. IEEE **51**, 1063 (1963).
[28] K. J. Nygaard, Phys. Letters **22**, 56 (1966).
[29] R. L. Taylor and S. B. Herskovitz, Proc. IEEE **53**, 657 (1965).

$\alpha(Ne_2^+)$ with gas temperature; however, the linear ranges ("f values") of the $1/n_e$-versus-t curves were rather small ($f\sim 4$) at temperatures greater than 300°K and the inferred values of α are therefore subject to large errors. Very recently, Kasner[3] has undertaken a similar study over the gas temperature range 295 to 503°K. He obtains sufficiently large linear reciprocal density ranges that his values should be quite accurate and, in addition, observes that the decay of Ne_2^+ wall current follows the volume electron-density decay over much of the afterglow. Kasner obtains a variation of $\alpha(Ne_2^+)$ as $T_{gas}^{-0.42}$, where $T_+=T_e=T_{gas}$, in excellent agreement with the present results.

The theoretical predictions concerning the expected dependence of α on T_e depend on which part of reaction (1) is the rate limiting step and on the details of the curve crossings between the XY^+ ion potential curve and the various unstable molecule states $(XY)_{unstable}^*$ involved in the recombination process. If every unstable molecule formed dissociates before auto-ionization (the first part of the reaction going to the left) can take place, then the initial capture step is rate limiting and an approximate dependence as $\sim T_e^{-1/2}$ is predicted.[30] If, however, stabilization of the reaction by dissociation is rate limiting, then a variation as $T_e^{-3/2}$ is predicted. Finally, if the unstable molecule potential curve crosses the molecular ion curve above its minimum, a threshold electron energy is required to initiate the reaction and α will at first *increase* with increasing T_e. Thus, the variation as $T_e^{-0.43}$ over the range $300°K<T_e<11\,000°K$ obtained in the present experiment suggests that dissociative recombination in neon is essentially rate-limited by the initial capture step.

The present experiment, therefore, appears to provide an accurate means of directly determining the absolute values of recombination coefficients and their dependence on electron temperature over a rather wide range. Inasmuch as one encounters conditions in the ionosphere where $T_e>T_+\simeq T_{gas}$, we are currently applying our techniques to studies of ions, such as N_2^+, which are of interest for ionospheric analyses under conditions which more accurately approximate upper-atmosphere conditions.

ACKNOWLEDGMENT

One of the authors (L.F.) wishes to acknowledge the support of the Joint Services Electronics Program while developing and carrying out some of the computer calculations.

APPENDIX A: ELECTRON HEATING CALCULATION

When the electron temperature is large compared to the gas temperature, the mean energy $\bar{\epsilon}$ may be calculated by use of Eq. (12), viz.,

$$\bar{\epsilon}=M\gamma^2F(z)/4\omega^2. \quad (12)$$

The graph $F(z)$ versus z is given in Fig. 6.

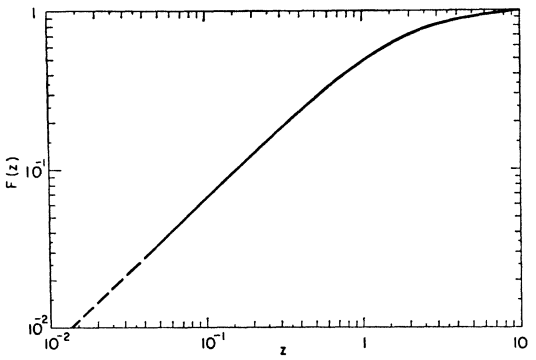

FIG. 6. The function $F(z)$ used to calculate the electron energy as a function of microwave heating field according to Eq. (12) or Eq. (13).

APPENDIX B: THE FUNDAMENTAL DIFFUSION LENGTH

The separation of variables in the solution of the diffusion equation, $\partial n_e/\partial t=D_a\nabla^2 n_e$, leads to a connection between the decay time constant of a given diffusion mode and the corresponding "diffusion length" for that mode.[31] In cylindrical geometry, the lowest or "fundamental" diffusion length is given by

$$1/\Lambda_f^2=(2.4/R)^2+(\pi/L)^2,$$

where R is the radius and L the length of the right circular cylinder.

In the present experiment, a cylinder terminated by conically tapered ends has been used to enclose the plasma (see Figs. 1 and 2). The cylinder radius is 1.5 cm, the untapered length is 8.6 cm and the length of each taper is 3.6 cm. Such a geometry does not yield a simple set of analytical spatial diffusion modes. Therefore, the computer solution of Eq. (5), with α set equal to zero, has been obtained to find the final exponential ("fundamental mode") diffusion decay time constant τ_f. From this and the value of D_a inserted in the computer program, one finds, for the conically tapered cylinder, $\Lambda_f\equiv(D_a\tau_f)^{1/2}=0.610$ cm. Thus, we find that, for lowest mode diffusion, this tapered cylinder can be well approximated by a right circular cylinder of the same radius but with an effective length $L_{eff}=9.1$ cm, that is, slightly longer than the untapered length of the actual container. Alternatively, one notes that the value of Λ_f for the tapered cylinder falls between that of an infinitely long cylinder, i.e., $R=1.5$ cm and $L=\infty$, for which $\Lambda_f=0.625$ cm, and that of right circular cylinder with $L=8.6$ cm (the untapered length of the present container), for which $\Lambda_f=0.607$ cm.

[30] D. R. Bates and A. Dalgarno, in *Atomic and Molecular Processes*, edited by D. R. Bates (Academic Press Inc., New York, 1962).

[31] M. A. Biondi and S. C. Brown, Phys. Rev. 75, 1700 (1949).